

Physical Characterization of Solid-Liquid Slurries at High Weight Fractions Using Optical and Ultrasonic Methods

Grant # 81964

6/15/04

Lead Principal Investigators:
L.W. Burgess and A.M. Brodsky
Center for Process Analytical Chemistry
University of Washington
Seattle, Washington
(206) 543-0579
Lloyd@cpac.washington.edu

Co-Investigators:
P.D. Panetta, R.A. Pappas, S. Ahmed, and B. Tucker
Pacific Northwest National Laboratory
Richland, Washington
(509) 372-6107
Paul.Panetta@pnl.gov

Graduate Student:
S.L. Randall
Center for Process Analytical Chemistry
University of Washington
Seattle, Washington
(206) 616-1492
sr33@u.washington.edu

Research Objective

The goal of this proposed work is to directly address the need for rapid on-line characterization of the physical properties of HLW slurries during all phases of the remediation process, from in-tank characterization of sediments to monitoring of the concentration, particle size, and degree of agglomeration and gelation of slurries during transport. Current technologies are not capable of characterizing the HLW waste stream without dilution. The results from this work will be utilized to develop new methodologies to characterize the HLW stream in-situ. There are three tasks: 1) develop new optical and acoustic scattering measurements to provide the fundamental science needed for successful device development and implementation, 2) develop theories that describe the interrelationship between wave propagation and the physical properties of the slurry, and 3) perform inversions of the theories and compare them with the experimental measurements to non-intrusively characterize slurries.

Research Progress and Implications

The interaction of high concentration slurries (up to 40 wt %) was studied utilizing both optical and ultrasonic fields. Slurries with mean particle sizes from ~0.01 μ m to 800 μ m

have been studied at concentration ranging from very dilute (< 1 wt %) to 40 wt %. The interrelationships between the attenuation, the direct backscattered field, and the diffusely propagating field have been studied. These fields are rich with information and unraveling their interrelationships will provide the robust methodology needed to characterize these HLW slurries and enhance the clean up process at the DOE facilities.

This integration of both optic and ultrasonic techniques is unique and exciting because it offers a combined methodology that exploits the best features of these two powerful techniques. The teaming of significant expertise in both experimental and theoretical optics (University of Washington) and in experimental and theoretical ultrasonics (PNNL) has provided a synergistic approach to coupling these complementary techniques. This combination of capabilities has allowed characterization to be performed over a broader range of particle sizes and concentrations than can be accomplished with existing techniques.

Optical Measurements

The optical measurements are based on the investigation of slurries with Optical Low-Coherence Reflectometry (OLCR). OLCR is a white-light interferometric technique that incorporates a broadband light source with a classical Michelson interferometer. In previous works¹ we have demonstrated that OLCR is an effective tool for nondestructive analysis of multiscattering systems.

During this FY our work has addressed many aspects of the OLCR system for slurry property monitoring. The probe design and development for the Optiphase OLCR instrument has been a non-trivial aspect of the instrumentation. The instrument design requires a triggering reflection, which we have chosen to be from the fiber end face without any contact from the sample. By adding the non-contact limitation, the fiber end face reflection can be used not only to trigger the instrumentation, but also to serve as a reference to correct for source fluctuations and allows us to track the matrix refractive index. The implications of this additional information are discussed below. For solid-liquid slurries, the probe has been designed to consist of standard single mode optical fiber, followed by a small air gap, and then a glass window angled at 8° relative to the fiber end face. This design results in triggering and reference reflections from the interface between the fiber end face and air, and the interface between air and the inside surface of the glass window. The reflection resulting from the outside surface of the glass window, which is in contact with the sample, will vary in amplitude based upon the refractive index difference between the window and the sample.

To confirm that the reflection from the interface of the outer surface of the probe window with the sample would vary with the refractive index difference between the window and sample, a series of solvents without scatterers and with refractive indices varying from 1.3283 to 1.4511 were analyzed with the new probe design. The probe design is illustrated as Figure 1 and the resulting OLCR profiles from the solvent series are shown in Figure 1B. The fourth reflection is a resonance effect which occurs due to the length of the air cavity within the probe. In later iterations, the air cavity length was decreased and the resonance reflection disappeared.

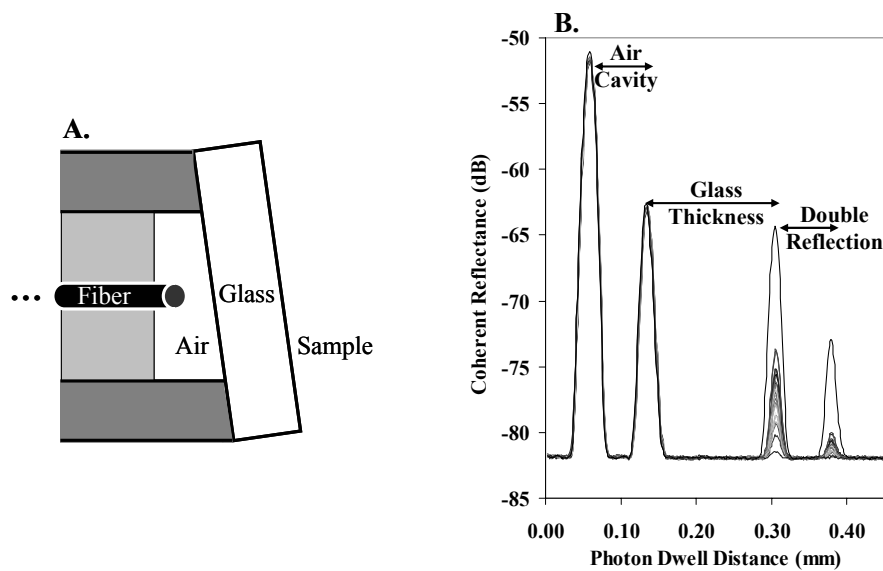


Figure 1. A) Simplified probe design consisting of bare single-mode fiber, the air cavity, and the glass window at an 8 degree angle. B) The resulting four reflections from a series of solvents with varying refractive indices.

The changing refractive index of the solvents, and thus the varying refractive index difference between the solvent and the window caused the amplitude of the third (and fourth) reflections to shift. The amplitude ratio of the reflection from the air-inside window interface to the reflection of the outside window-sample interface can be related to the refractive index of the sample, as shown in Figure 2. The refractive index can be directly related to the concentration and size of dispersed material of known refractive index, and can be diagnostic during agglomeration as particles transition from one scattering regime to the other. This feature will aid us in deconvoluting dynamic changes in the slurry system.

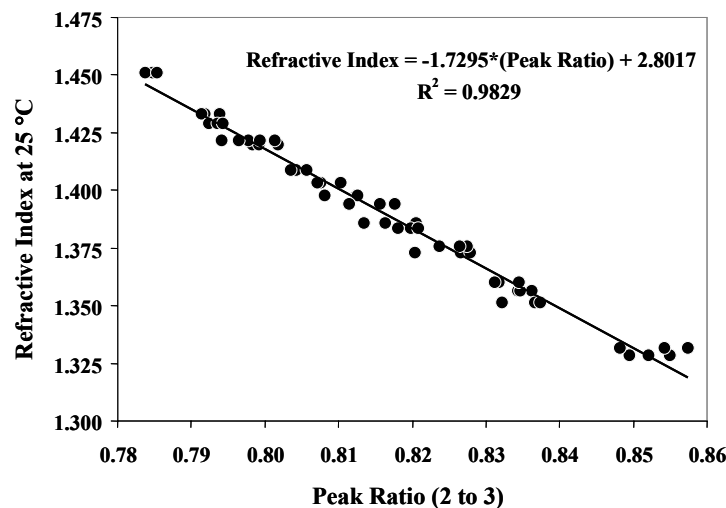


Figure 2. Linear relationship between peak ratio and refractive index for a series of solvents.

The optical experimental work focused upon using standard, monodispersed polystyrene nanospheres purchased from Duke Scientific Corporation to act as a model system for theory and experimental development over a large dynamic range of particle sizes. The shape and intensity of the OLCR profiles changes as the measured particle size

transitions from the Rayleigh regime to the Fraunhofer regime, as shown in Figure 3. One of the most interesting results of this work is the observation of so-called Mie resonances when the particle radii of a randomly distributed system are comparable with the wavelength of light. This non-monotonic oscillation of backscattered intensity is dependent upon optical parameters, such as dielectric contrast between the medium and the particles², and is shown in Figure 4A.

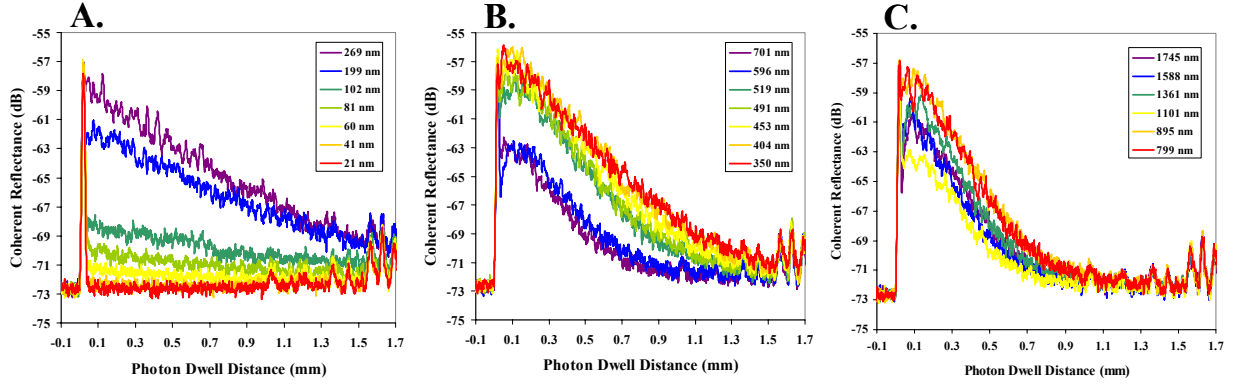


Figure 3. OLCR profiles for polystyrene sphere standards for diameters A) 21 nm to 269 nm, B) 350 nm to 701 nm, and C) 799 nm to 1745 nm.

Advances in the optical theory of multiple scattering have been made, specifically to begin to extract information pertaining to system properties, such as particle size, concentration, and polydispersity, from all regions of the OLCR profile. Theoretical estimations of the experimental amplitude oscillation are shown as Figure 4B and are described in the following equation:

$$\text{Log } I_T - \text{Log } I_0 = \text{Log} \left(1 + C\rho_0 \left[\frac{[\cos(y)]}{y} - \frac{([\sin(y)]/y)^2}{\left(\frac{1}{2} - [\sin(y)]/y + [1 - (\cos(y)]/(y^2))^2 \right)} \right] \right) \quad (1)$$

where $\text{Log } I_T$ is the total signal, $\text{Log } I_0$ is the baseline signal, C is an instrumentally-based constant, ρ_0 is the volume fraction of particles in the studied media, $y = 4\pi R\Delta\epsilon_M/\lambda$ with R as the particle radius, Δ as the optical contrast between the particles and media, ϵ_M is the dielectric function of the media, and λ as the wavelength of light in a vacuum. The described results are interesting as a step toward advancement in the understanding of the theoretically and practically important problem of wave propagation in multiscattering random media. A manuscript has been submitted to describe both the experimental and theoretical Mie resonance results³.

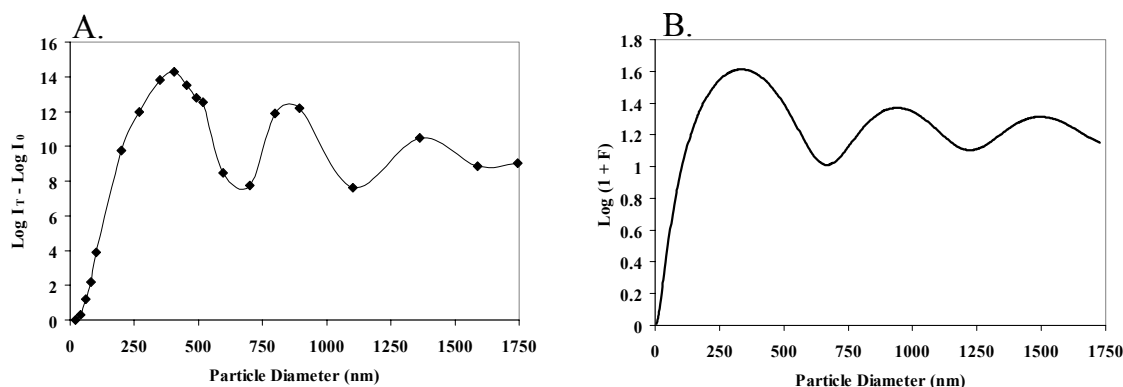


Figure 4. A) Oscillation in signal intensity from 1.4 to 1.6 mm resembles Mie resonances with increasing particle size. B) Theoretical expression including $C=11307/\Delta^2$, with $\Delta=1.35 \pm 0.1$ to describe the experimental data.

In order to demonstrate OLCR measurement capabilities in a more complex and realistic matrix, measurements were performed upon bimodal mixtures of individual polydispersed alumina suspensions. The four alumina samples were a subset from the AZ-101/102 surrogate slurry developed by Golcar et al. [2000] and shown as Table 2. These were easily distinguishable from each other when measured individually at 30 wt %, and covered a large dynamic range of mean particle sizes (0.25 microns to 55 microns). The 55 micron and the 0.25 micron alumina components were mixed in ratios of 1:0, 9:1, 3:1, 1:1, 1:3, and 0:1, respectively, to produce average particle sizes of 55 microns, 52 microns, 41.3 microns, 27.6 microns, 13.9 microns, and 0.25 microns. The slurry concentrations were held constant at 30 wt %. The resulting OLCR profiles are shown as Figure 5. Distinction can be made between the bimodal mixtures and the trend of changing average particle size can be easily followed through the profile amplitude. This result is very exciting and extremely encouraging towards our ability to track changing dimensions in a complex, polydispersed, multi-modal surrogate slurry.

Table 2. AZ-101/102 Slurry Simulant Composition. The HiQ-10 Alumina Mean Volume PSD should read 55 microns instead of 0.0028-0.004 microns.

Solids Components					
Compounds Bearing:	Wt %	Mineral Phase	Powder Grade	Mean Volume PSD (Distribution)	Wt %
Iron	58	Hematite	Iron Oxide No: 07-5001	22 μm	17.400
			Red Iron Oxide No: 07-3752	2-3 μm	29.000
			Synthetic Red Iron Oxide No: 07-7568	0.6 μm	11.600
Aluminum	24	Boehmite	HiQ-10 Alumina	0.0028-0.004 μm	7.200
		Gibbsite	C-231 Ground White Hydrate	14 μm (broad)	8.400
			SpaceRite S-23 Alumina	7.5 μm (broad)	5.040
			SpaceRite S-11 Alumina	0.25 μm (narrow)	3.360
		Gibbsite/Boehmite Ratio: 2.33			
Zirconium	13	Zirconium Hydroxide	Zirconium Hydroxide; Product Code: FZO922/01	15 μm	13.000
Silicon	5	Nepheline	Spectrum A 400 Nepheline Syenite	10 μm	5.000
Supernatant Components					
Component	Concentration (M)		Concentration (g/L)		
NaOH	0.8		32		
NaNO ₃	1.0		85		

The alumina component will serve as an excellent surrogate waste model for both static and dynamic studies. We have developed a greater understanding of how the complete surrogate slurry will act through the analysis of bimodal polydispersed alumina mixtures. Gelation, agglomeration, and sedimentation have all been shown to occur by adjusting parameters of the alumina system (i.e. pH, flow rate, temperature) and will be systematically studied in our future work.

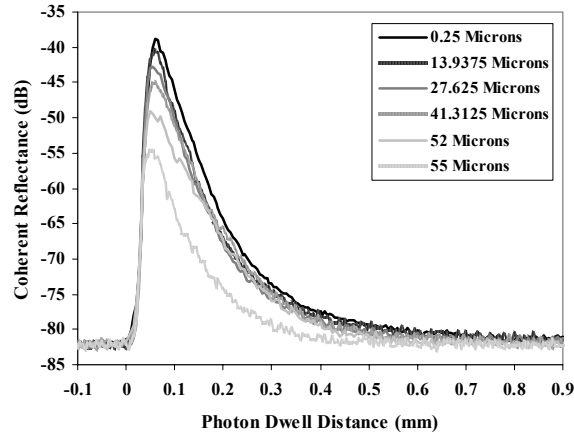


Figure 5. OLCR profiles measured from bimodal polydispersed alumina slurries.

Overall, we have made significant progress in the analysis of signals obtained from multiple scattering events. We have observed the appearance of Mie resonances, a non-monotonic oscillation of backscattered intensity dependent on optical parameters, over the interval where radii are comparable to the wavelength. The results above clearly indicate that it is possible to extract important static and dynamic parametric information from dense scattering systems with OLCR. Between the refractive index information, fluctuation distributions, amplitude variation, and decay rate, we should be able to extract characteristic information about particle systems. If all the variables are changing simultaneously, we hope to further resolve the parameter convolution by utilizing the synergy of the project and incorporating information from the ultrasound data.

However, these data do not yet reveal how we may be able to extract effects such as gross polydispersity, particle geometry, variable viscosity, or widely variable dielectric contrast that will be present in the slurries and colloidal systems of interest to the DOE. Our challenge will be to select well-characterized surrogate systems that will allow us to study these processes and aid theoretical development.

Ultrasonic Measurements

During this FY PNNL has been a developing ultrasonic measurement methodology to characterize solid liquid suspensions at high concentrations. A schematic of the measurement system is shown in Figure 6a with representative signal used for calculating the attenuation and speed of sound in Figure 6b, the backscattering in Figure 6c, and the diffuse field in Figure 6d. The measurement cell is composed of a ring with opposing transducers to send and receive the ultrasonic fields. The speed of sound is simply a

measure of the transit time across the chamber and the attenuation is a measure of the amount of energy lost due to scattering and absorption as the sound traverses the chamber. The backscattering is a measure of the amount of ultrasound that is returned to the transmitting transducer. The diffuse field develops after the ultrasonic field has undergone many scattering events with the particles in the fluid and the walls of the chamber. For the attenuation, backscattering and the diffuse field, the Fourier amplitude is calculated to study the frequency dependence of these parameters. The effects from the measurement system and the transducer are removed from the received signal by utilizing an appropriate reference signal. Details can be found in publications that resulted from this work.

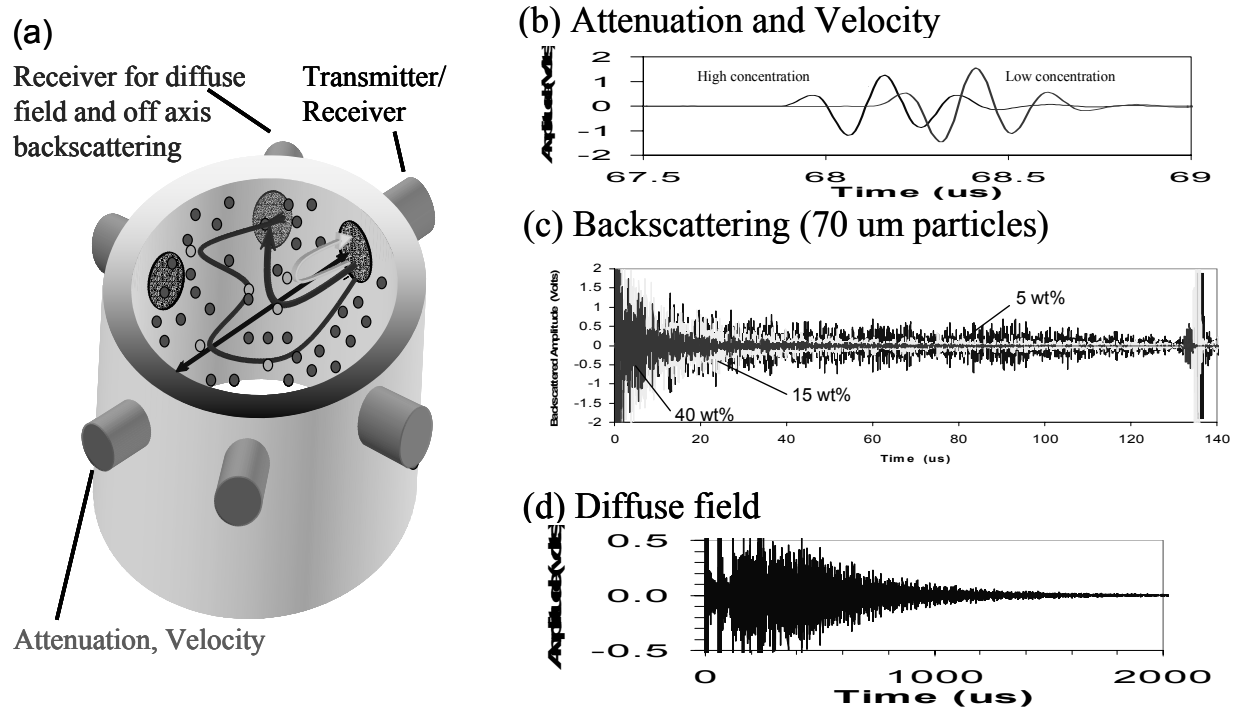


Figure 6. (a) Schematic of ultrasonic measurement apparatus, (b) through transmitted RF signal for attenuation and velocity determination, (c) directly backscattered signal, and (d) diffuse field signal.

Results from the methodologies under development in this project are shown in Figure 7, where the attenuation as a function of frequency is plotted for 70 um glass spheres in water. The experimental measurements favorably compare with theoretical predictions from algorithms generated from this project. One of the key aspects of the attenuation is the dependence on frequency. Specifically, the dependence is controlled by the dominant attenuating mechanisms which are (1) the heat loss due to the friction between the viscous fluid and the particles as they move through the slurry, (2) the energy required to accelerate and decelerate the particle as it oscillates, and (3) the scattering of sound out of the propagating field. The attenuation for the glass spheres in water is dominated by the scattering of the sound field at the water particle interfaces. The frequency response is consistent with the attenuation entering the multiple scattering regime, where the attenuation increases with frequency to the 4th power.

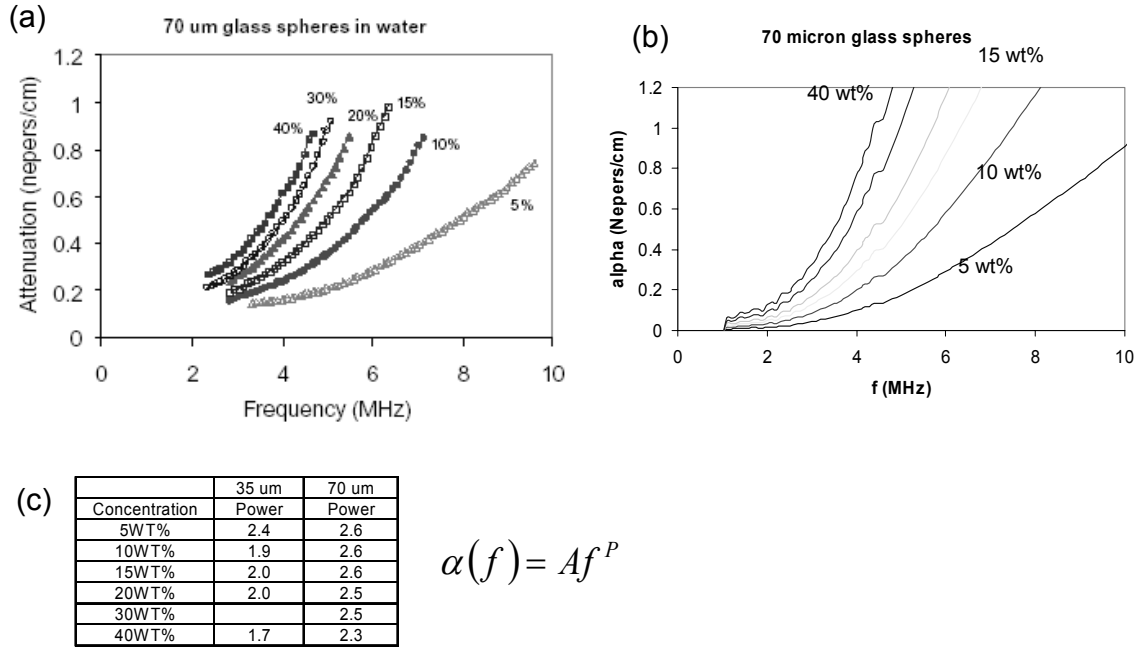


Figure 7. Attenuation as a function of frequency for 70 um glass spheres in water (a) experimental measurements, (b) theoretical predictions, and (c) the frequency response of the experimental data.

One of the unique measurements that has been developed during this project is the backscattering measurement where the ultrasonic field that is scattered directly back to the transmitting transducer is analyzed. Specific results for the same glass spheres in water are shown in Figure 8 for the experimental and theoretical predictions of the backscattering. Further development is underway to incorporate the particle-particle interactions to the backscattering which is expected at high concentrations. Another important aspect of the backscattered field as shown in Figure 6c is the characteristic decay in amplitude as a function of time. This decay is a measure of the energy loss due to the attenuating mechanisms previously discussed, but less is known about these fields. A part of this project, we are advancing this understanding to better utilize the backscattering to characterize solid liquid suspensions. For example, Figure 9 shows the decay rate of the 5 MHz component of the backscattering as a function of concentration of glass spheres in water. The decay rate of the backscattering as a function of particle size is shown in Figure 9b for polystyrene like particles. These data show that the backscattering effectively scales with concentration even up to very high solids loading and with particle size from sub micron particles to the several 10's of micron particles. These results represent new advancements in the understanding and applications of the ultrasonic backscattering to characterize high concentration solid-liquid suspension.

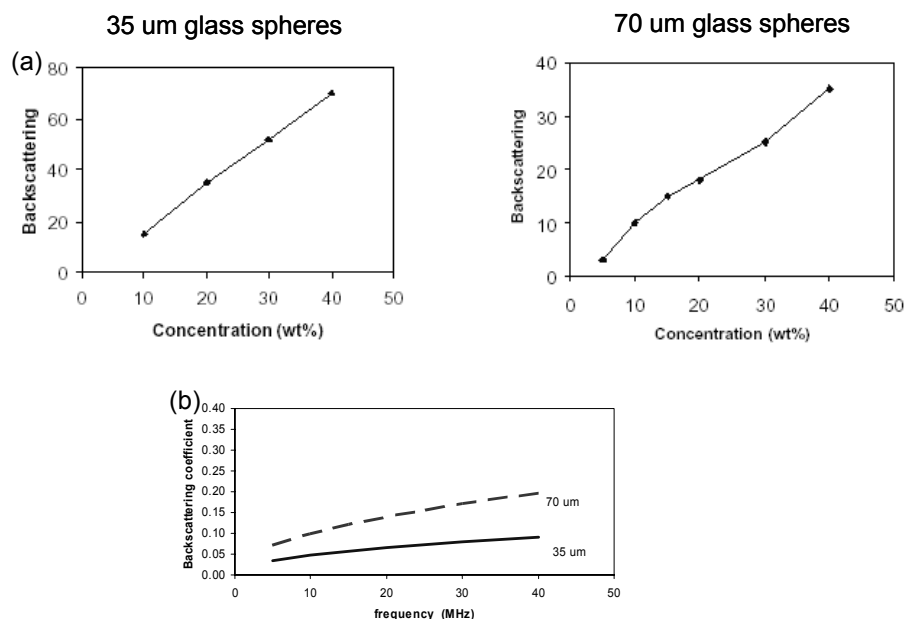


Figure 8. The resultant backscattering as a function of concentration from 5-15 us region after correcting for attenuation losses at 5 MHz and (b) theoretical predictions.

Current results indicate that the ultrasonic measurements are very sensitive to both particle size and concentration. We have focused ultrasonic backscattering measurements that have the best opportunity to provide quantitative results at the high concentrations expected to occur in the waste remediation process. Results on the aluminum oxide subset of the stimulant for AZ101/102 tank waste have been performed with preliminary results have been previously reported.

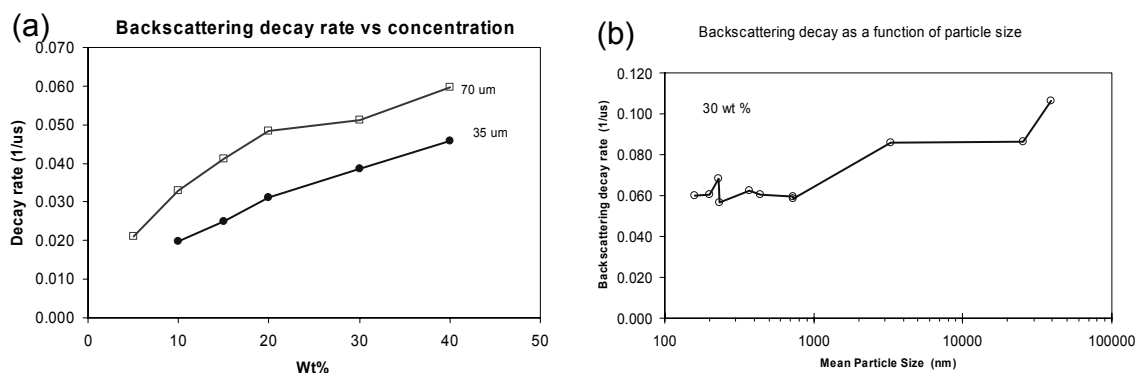


Figure 9. The backscattering decay rate (a) as a function of concentration for the 35 and 70 um glass spheres in water and (b) as a function of particle size for a solid-liquid suspension with properties similar to polystyrene in water.

The backscattering and diffuse field measurements are especially appealing because of the relative simplicity of the measurement and the theoretical description of the scattering processes. Future plans include extending existing theories to include multiple scattering

and particle-particle interactions, which occur at high concentrations. It will then be possible to compare the developed acoustic and optical theory with the experimental results. The main goal of the calculations is to determine the expressions which will allow a solution to be found for the inverse problem—characterization of studied media (including dense slurries) by acoustic scattering data.

Planned Activities

Upcoming work will include evaluation of polydispersed standard systems for both the optical and acoustic methods simultaneously in the same measurement chamber. The polydispersed systems will be formulated by mixing several of the previously analyzed monodispersed systems to provide average, and known, particle characteristics. Additional studies will be performed upon individual, broadly dispersed slurry surrogate components. We will also focus on the surrogate slurries for the Hanford tank waste. Upcoming work will include the variation of solvents and pH for the alumina slurry components to follow phase transitions, such as agglomeration and gelation. Eventually we will analyze a complex matrix composed of multiple surrogate components with both optical and acoustic techniques.

Publications

Project research to this point has resulted in numerous presentations at the International Particle Size Analysis 2003 Conference (Harrogate, UK), at the Center for Process Analytical Chemistry Semi-Annual Meetings, at the Review of Progress in Quantitative Nondestructive Evaluation 2002 and 2003, at the International Forum for Process Analytical Chemistry 2004, at the IEEE Instrumentation and Measurement Technology Conference 2003, and at the National American Chemical Society Conference in Anaheim 2004. Publications as a result of this research include Brodsky and Burgess [2003], Randall et al. [2003], Randall et al. [2004] submitted, Panetta et al. [2003], Panetta et al. [2004] in press, and will also include the Ph.D. Dissertation of Summer Lockerbie Randall.

References

1. Randall, S.L., A.M. Brodsky, L.W. Burgess, and R.L. Green. 2003. "Optical Low-Coherence Reflectometry for Nondestructive Process Measurements," 29th Annual Review of Progress in Quantitative Nondestructive Evaluation (QNDE), Bellingham, WA.

Thurber, S.R., A.M. Brodsky, and L.W. Burgess. 2000. "Characterization of Random Media by Low Coherence Interferometry." *Applied Spectroscopy*, 54(10), 1506-1514.

Brodsky, A., Thurber, S.R., and L.W. Burgess. 2000. "Low-Coherence Interferometry in Random Media I. Theory." *Journal of the Optical Society of America A*, 17(11), 2024-2033.

- Thurber, S.R., Burgess, L.W., A. Brodsky, and P.H. Shelley. 2000. "Low-Coherence Interferometry in Random Media II. Experiment." *Journal of the Optical Society of America A*, 17(11), 2034-2039.
2. Brodsky, A. and L. Burgess. 2003. "Theoretical Study of the Coherent Backscattering of Light by Disordered Media." *Intl. J. Modern Physics B*, 17(3), 337.
3. Randall, S.L., A.M. Brodsky, and L.W. Burgess. 2004. "Manifestation of Mie Resonances in Light Scattering from Multiscattering Media." *Submitted to Optics Letters*.
4. Golcar, G.R., K.P. Brooks, J.G. Darab, J.M. Davis, and L.K. Jagoda. 2000. Development of Inactive High Level Waste Envelope D Simulants for Scaled Crossflow Filtration Testing, PNWD-3042.
5. Panetta, P.D., B.J. Tucker, R.A. Pappas, and S. Ahmed. 2003. "Characterization of solid liquid suspension utilizing ultrasonic measurements", 29th Annual Review of Progress in Quantitative Nondestructive Evaluation.
6. Panetta, P.D., B. Tucker R. A. Pappas, and S. Ahmed. "Characterization of Solid Liquid Suspensions Utilizing Ultrasonic Measurements" IEEE Instrumentation and Measurement Technology Conference (in press)